Free convection along pumped active mirror amplifying medium and its impact on laser wave propagation.

Hugo Chesneau[1,*], *and Sébastien* Montant[1]

[1] Commissariat à l'Energie Atomique et aux Energies Alternatives, Centre d'Etudes Scientifiques et Techniques d'Aquitaine, F-33116 Le Barp, France.

Abstract. Using COMSOL Multiphysics, we simulate free convection along a pumped active mirror amplifying medium. We study the induced boundary layers and how it affects the wave front propagation. To comfort our simulations, we set up a Mach-Zehnder interferometer to characterize and measure the local variation of air refractive index and temperature.

1 Introduction

Active mirrors amplification scheme is a solution to enhance laser beam mean power with a lower number of passes compared to thin disk amplifier [1]. The rise of mean power increases the thermal load. Hence, it induces thermal effects issues like free thermal convection in air.

To quantify these effects, we perform numerical and experimental investigations. Numerically, we simulate the heat transfer within the pumped active mirror (which can be referred to as the disk in the text) and in the air and we observe the induced thermal boundary layer along it. In order to validate our numerical model, we set up a Mach-Zehnder interferometer (MZI) to observe and measure local variation of both air refractive index and temperature. From the resulting interferograms we compare numerical and experimental results. Finally, we use an Algebraic Reconstruction Technique (ART) [2] to compute the 3D refractive index field and temperature.

In what follows, we describe the physical and numerical system, the experimental system and the chosen method for the 3D reconstruction.

2 Physical and numerical system

We describe the numerical system on an orthonormal Cartesian basis with the unit vectors $(\mathbf{e}_x, \mathbf{e}_y, \mathbf{e}_z)$. The fluid flow is considered as incompressible, and we make the assumption of the Boussinesq approximation; only the density of the fluid changes with temperature. To have a universal numerical model, we used only dimensionless variables. We take the following characteristic variables. D the active mirror diameter, $u_T = (g\beta q_w D^2/k)^{1/2}$ and $p_T = \rho_0 u_T^2$ respectively the thermal velocity and pressure. $\Theta = (T - T_a)k/(q_w D)$ a relative temperature to the ambient one, $Q_c = q_w/D$ a source term, and the dimensionless Grashof and Prandtl numbers which are denoted $\mathrm{Gr} = g\beta D^4 q_w/(k\nu^2)$ and $\mathrm{Pr} = \rho_0 \nu C_p/k$. With $\mathbf{g} = g\mathbf{e}_x$ the gravity, β the thermal expansion coefficient, ν the kinematic viscosity, k the thermal conductivity, ρ_0 the density, C_p the isobaric heat capacity and q_w a surface heat flux. All these quantities are related to the air at room temperature (20°C). The dimensionless governing system of equations is:

$$\nabla \cdot \mathbf{u} = 0 \tag{1}$$

$$(\mathbf{u} \cdot \nabla)\mathbf{u} = -\nabla p + \Theta \mathbf{e}_x + \mathrm{Gr}^{-\frac{1}{2}} \nabla^2 \mathbf{u} \tag{2}$$

$$(\mathbf{u} \cdot \nabla)\Theta = \mathrm{Gr}^{-\frac{1}{2}} \mathrm{Pr}^{-1} \nabla^2 \Theta + \mathrm{Q_c} \tag{3}$$

These equations are respectively, the mass, the momentum and the energy conservation. In our experimental conditions $\mathrm{Gr} \approx 10^6$ and $\mathrm{Pr} = 0.7$.

3 Experimental system

We set up a MZI to probe the heated air in front of the disk as shown in Figure 1.

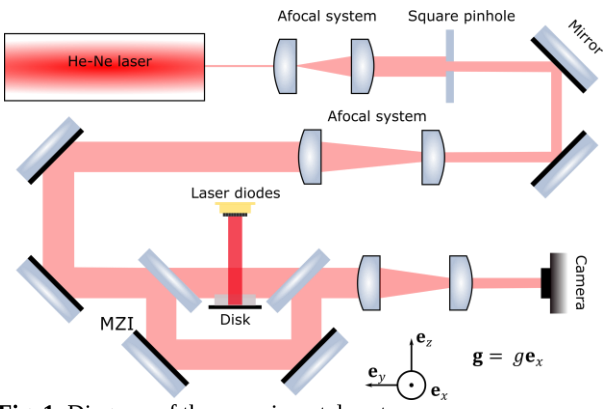

Fig. 1. Diagram of the experimental system.

To capture the whole behaviour of the boundary layers, we use a square-shaped He-Ne laser beam. The incident gaussian beam is magnified sixteen times

* Corresponding author: hugo.chesneau@cea.fr

through a first afocal system with two plano-convex (PC) lenses. Then, it is shaped with a square pinhole, expanded three times with another set of PC lenses and imaged in front of the active mirror in one of the interferometer arm. Finally, we use a last pair of PC lenses to decrease the size of the beam by a factor three and we image it on a camera. The active mirror is pumped with laser diodes at $\lambda_d \sim 800\text{nm}$, delivering $E_d = 1.6\text{J}$ at a frequency of $f_d = 4\text{Hz}$ with $\tau_d = 400\mu\text{s}$ pulses. We depict on Figure 2 the typical results we can get at room temperature and with the pumped active mirror. Figure 2 (b) clearly highlights the fringe shift resulting from the thermal boundary layer in front of disk and the plume above it.

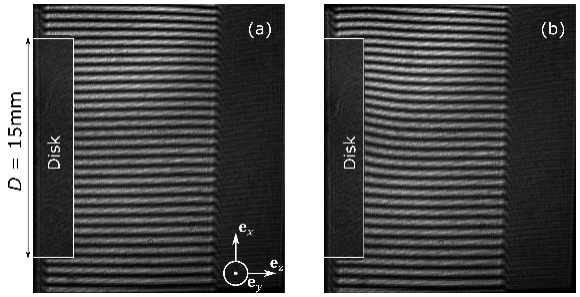

Fig. 2. Snapshots of the interference patterns obtained with the MZI (a) at room temperature and (b) with the pumped disk.

Once we have both interference patterns, we are able through Fourier analysis to compute the phase shift induced by the refractive index gradient [3]. As a thumbnail sketch, it consists in (i) Fourier transform the images, (ii) selecting and filtering the spatial frequency of the interferences and (iii) invert Fourier transform the filtered spectrum to get the wrapped phase of the interference pattern. Finally, (iv) we unwrapped the latter [4] to compute the phase shift as displayed in Figure 3 (b).

Thereafter, we perform the same experiment for different angles with the $\mathbf{e}_y$ axis to reconstruct the refractive index field with a Simultaneous Iterative Reconstruction Technique (SIRT)[5], which is a kind of ART. The method can be sum up in a few steps to. First, we write the phase shift induced by the integration of the spatially varying refractive index as a discrete ray-sum equation; each pixel of the camera is considered as the result of a single beam. Meaning that, the continuous equation becomes:

$$\varphi_{\text{ij}} = \sum_{ij} \frac{2\pi}{\lambda}\left(n_{ij} - n_0\right) w_{ijnm} = \sum_{ij} f_{ij} w_{ijnm} \quad (5)$$

With λ the laser beam wavelength, L the propagation distance and n_0 the unperturbed refractive index. The indexes (i,j) represent the coordinates of the grid on which we reconstruct the field, n is for a given angle of projection and the index m denotes each ray (pixel). f_{ij} is called the perturbation function and w_{ijnm} is a weight matrix which is the distance covered by the m^{th} beam for the n^{th} projection in each (i,j) cell.

$$\text{f}_{\text{ij}}^{(q+1)} = f_{ij}^{(q)} + \alpha \frac{\sum_{mn} w_{ijmn} \times \frac{\varphi_{mn} - \sum_{ij} w_{ijmn} f_{ij}^{(q)}}{\sum_{ij} w_{ijmn}}}{\sum_{mn} w_{ijmn}} \quad (6)$$

The letter (q) denotes the q^{th} iteration. α is a relaxation coefficient for which the iterative algorithm is stable when $0 < \alpha \leq 2$.

4 Preliminary experimental results and conclusion

We show on Figure 3 a first comparison between numerical (a) and experimental (b) phase shift. We retrieve similar boundary layer shape and the same amplitude of phase shift in both cases. One could also note that we likely did not pump the active mirror at his center regarding the position of the minimum experimental phase shift.

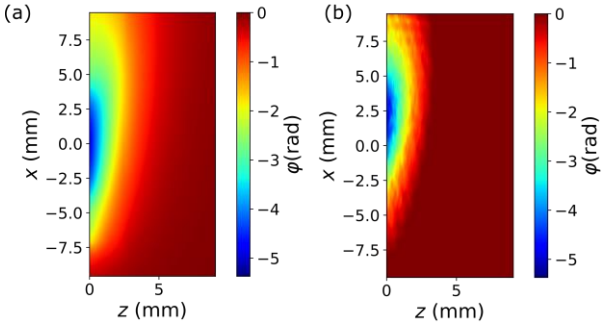

Fig. 3. Numerical (a) and experimental (b) calculated phase shift for a probe beam propagating along $\mathbf{e}_y$ axis.

5 Conclusion

We fully characterised numerically the boundary layers and the refractive index gradient induced by the active mirror pumping. We successfully compared the resulting phase shift computed from numerical and experimental results. Finally, we plan to perform more experiments with different viewing angles, to be able to reconstruct the 3D refractive index field.

This work was partly supported by the Conseil Régional de Nouvelle Aquitaine and the European Union through the project LEAP - Axes B et C (contracts CPER #16004205 and #DEE21-04-2019-5131820 and ERDF #2663710 and #3404410).

References

1. D. C. Brown, J. H. Kelly, J. A. Abate, IEEE J. Quantum Elect. **QE-17**, 9, 1981.
2. A. H. Andersen, A. C. Kak, Ultrasonic Imaging **6**, pp. 81-94, (1984)
3. D. J. Bone, H.-A. Bachor, R. J. Sanderman, Appl. Opt. **25**, 1653, (1986)
4. M. A. Herraez, D. R. Burton, M. J. Lalor, M. A. Gdeisat, Appl. Opt., **41**, 35, 2002.
5. G. Golovin, S. Benerjee, J. Zhang, S. Chen, C. Liu, B. Zhao, J. Mills, K. Brown, C. Ptersen, D. Umstadter, Appl. Opt. **84**, 11, (2015)